

Simulations of Axially Loaded Straight Aluminium Profiles with Random Geometric Imperfections

Ø. Fyllingen¹, O.S. Hopperstad, M. Langseth
Structural Impact Laboratory (SIMLab)
Department of Structural Engineering
Norwegian University of Science and Technology
Rich. Birkelands vei 1A, NO-7491 Trondheim, Norway

Abstract

Stochastic simulations of square aluminium tubes of 6060 T6 aluminium alloy subjected to axial crushing have been performed in LS-DYNA and compared to existing experiments. The main variables of the experimental study were the extrusion length, the wall thickness and the impact velocity. Three different buckling modes were observed; progressive buckling, a transition from progressive to global buckling and global buckling.

In the present study it has been investigated if it is likely that geometric imperfections modelled by assumed Gaussian random fields can explain the experimentally observed behavior. Variation of the random field parameters by use of a factorial design resulted in variations in especially the buckling modes and consequently the average force.

Introduction

It is a challenging task to simulate buckling of straight profiles because only small variations in the boundary conditions, material properties and geometry can lead to substantial variations in the behavior and consequently the energy absorption. According to Marczyk [3] the inclusion of random fields may increase the degree of realism in the response mechanism of a model and can in some cases explain strange patterns of behavior that can not be estimated by conventional finite element models.

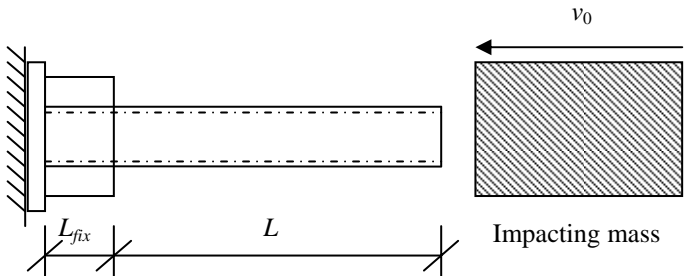
In this study a simple component has been simulated based on experimental tests performed by Jensen et al [1]. In their study straight square thin-walled aluminium members in 6060 T6 alloy were subjected to axial crushing. Components of different lengths and wall thicknesses were tested at varying impact velocities. As the length of the components increased the components became less efficient as energy absorbers. The main objective with the present study is to use random fields to model the tests performed by Jensen et al [1] with focus on the observed deformation modes. As the simulations are quite computational expensive, only one wall-thickness of the profiles has been chosen for the comparison.

¹ Corresponding author: Tel: + 47-73-59-47-00; fax: +47-73-59-47-01.
E-mail address: orjan.fyllingen@ntnu.no

Experiments

In the experiments performed by Jensen et al [1] and Jensen [2] the transition between progressive and global buckling of axially loaded square thin-walled aluminium extrusions in alloy AA6060 temper T6 was studied by quasi-static and dynamic tests. Profiles of different lengths and thicknesses were tested at different impact velocities. However in the present study it will be focused on the components with a wall thickness (t) of 3.5 mm subjected to an impact velocity (v_0) of 13 m/s.

Table 1. Test specimen geometry and support conditions for the dynamic tests (Jensen et al [1]).

Test set-up	Parameters
	Wall thickness (t) 3.5 mm
	Free length (L) 798– 1598 mm
	Impact velocity (v_0) and mass 13 m/s and 1400 kg

The test program is presented in Table 1. The width (w) of the extrusions was kept constant at a nominal value of 80 mm and the free length (L) varied between 798 mm and 1598 mm. A pendulum accelerator was used to accelerate a trolley of 1400 kg against the free end of the specimens. At the distal end the specimens had a clamped support. The length of this support (L_{fix}) was 100 mm.

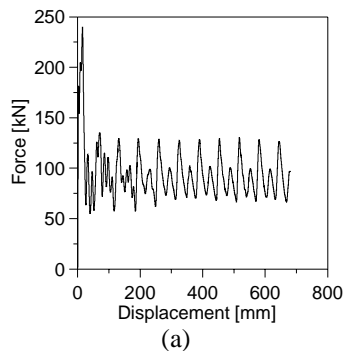


Figure 1. Profile D1-10, $L = 1201$ mm, $v_0 = 13$ m/s, $t = 3.5$ mm: (a) force versus deformation, (b) deformed geometry (Jensen [2]).

Progressive buckling and a transition from progressive to global buckling were experienced when varying the length of the profiles. The shortest profiles experienced a progressive buckling mode, see Figure 1. An initial peak was observed in the force-displacement curve, followed by oscillations around an average force level.

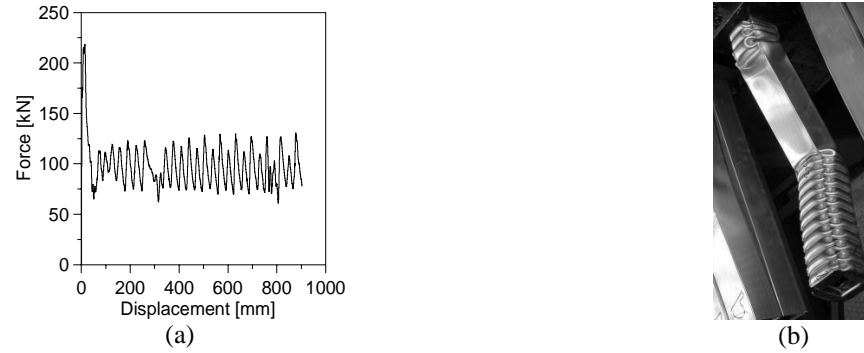


Figure 2. Profile D1-6, $L = 1598$ mm, $v_0 = 13$ m/s, $t = 3.5$ mm: (a) force versus deformation, (b) deformed geometry (Jensen [2]).

When the length was increased, one profile experienced a transition from progressive to global buckling, see Figure 2. The profile started to fold progressively and after some deformation a transition from progressive to global buckling with large lateral displacements occurred. In Figure 2 (a) the initial peak force is followed by oscillations in the force level as in the case of a progressive buckling mode, but the force would have dropped significantly when the transition to global failure occurred if the profile had deformed further.

Table 2. Results from impact tests, $v_0 = 13$ m/s, $t = 3.5$ mm (Jensen et al [1]).

L [mm]	P_m [kN]	Mode ¹
798	104	P
880	91	P
1120	95	P
1201	94	P
1358	96	P
1380	-	P
1440	86	P
1598	98	T

¹ G = global buckling, P = progressive buckling and T = transition.

The experimental results are presented in Table 2. The profiles with L equal to and shorter than 1440 mm experience progressive buckling, whereas the profile with L equal to 1598 mm experience a transition from progressive to global buckling. The average force P_m was calculated by dividing the energy absorbed by the total displacement.

Finite Element Model

Before a numerical simulation of the impact loaded profile can be carried out a simplified model has to be developed, the governing equations have to be formulated and a decision has to be made about how the governing equations should be solved in space and time. In problems involving impacts and large deformation the explicit finite element codes are preferable because of both CPU-time efficiency and robustness. All the simulations presented here have been performed with the FEM-code LS-DYNA.

Stochastic FEM simulations of impacts are quite time consuming. Thus considerations have to be made about what simplifications can be done in order to reduce the CPU-time. One of the major simplifications is the use of shell elements. The LS-DYNA default shell element, Belytschko-Tsay (type 2), which is quite robust and efficient, has been used in the present study. The number of integration points through the thickness was set to 5 and the option membrane causing thickness change was chosen. The elements were approximately square shaped and 16 elements over the width of the extrusion seem to describe the observed deformation modes satisfactorily.

The sample mean of the width (w) of the square profiles was 79.8 mm. Further the profiles had a small curvature at the corner which was ignored in order to reduce the CPU-time. The impactor was modelled as a 400 mm x 400 mm plate with thickness of 2 mm with one layer of solid elements and rigid body material. The clamped part of the member which is 100 mm was modelled with all rotational and lateral degrees of freedom fixed. The axial degree of freedom was fixed only at the bottom row of nodes. The component was unrestrained elsewhere. Material model 103 [7] in LS-DYNA was applied with parameters obtained from material tests [1]. Strain rate effects were not considered.

To account for contact between the impactor and the profile, automatic surface to surface contact was used. The friction coefficient between dry aluminium and steel is 0.61 according to Hallquist [8]. The self contact in the profile was modelled by use of single surface contact with a static friction coefficient of 1.05 [8]. The dynamic friction was set equal to the static friction for both contacts.

Gaussian random fields or transformations of them are the most widely used random fields in general. As no proper measurements of the geometric imperfections of the profiles in the study by Jensen et al [1] have been performed, no exact representation of a random field model is possible. However, in the present study a random field model will be assumed. One of the simplest random fields is a stationary Gaussian random field. The effect of changing the parameters of this field will be investigated within the limit of production tolerances.

A Gaussian random field may be represented by a mean and a covariance function. Since the field is assumed to be stationary both the mean and covariance will be independent of translations in space. The Gaussian covariance function will be used in the present study:

$$C(\tau) = \begin{cases} \sigma^2 \exp\left(-\left(\frac{\tau}{R}\right)^2\right) & \text{if } \tau > 0 \\ \sigma^2 & \text{otherwise} \end{cases} \quad (1)$$

where τ is the distance between two locations, the quantity σ^2 is called the sill and R will be referred to as the range parameter. The sill is similar to the variance for a univariate distribution, while the range parameter controls the degree of covariance between two locations. In order to generate anisotropic fields coordinate transformation is applied. A direction of maximum range and an anisotropy ratio ϕ have to be chosen. ϕ is defined as the ratio between the ranges of the directions with greater and smaller continuity, i.e. the ratio between maximum and minimum ranges [6]. The coordinates are first transformed to the isotropic space, simulation is done and

then the coordinates are back-transformed. More details about random fields may be found in Banerjee et al [4].

There exist several codes for random field sampling. In the present study the code R [5] with the package geoR [6] is used. The function $\text{grf}(\cdot)$ generates samples of Gaussian random fields for given covariance parameters.

Before the statistical variables and fields can be defined, it is convenient to define the orientation of the profile in a Cartesian co-ordinate system, see Figure 3. The location of the origin is such that the ends of the profile will lie at $z = \pm(L + L_{fix})/2$.

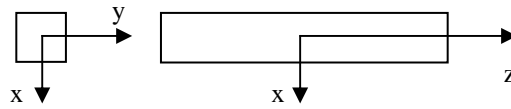


Figure 3. Orientation of the profile in a Cartesian co-ordinate system.

According to Jensen [2] the tolerances for an industrial bar are about $w/200$ and $(L+L_{fix})/2000$ for the local and global imperfections, respectively. The local imperfections will be represented by 4 independent random fields, one field on each of the extrusion walls. The field values will be generated at the same locations as the finite element nodes. The global geometric imperfections will be represented by two independent random fields generated on two perpendicular planes. One way to look at it is to generate the field on one wall in the same way as for the local imperfections and then give the parallel wall the same imperfections in the same direction. The perpendicular walls will be given a sideways imperfection equal to the imperfections at the corners. σ^2 and R are taken as 1.0^2 mm^2 and 2000 mm , respectively, and the field will be isotropic in all the simulations. In order to not exceed the tolerance a new sample is generated if the limit $(L+L_{fix})/2000$ is exceeded.

Based on measurements of the thicknesses at each wall for the profiles and some simplifications it was found that the thicknesses may be represented by a four dimensional multivariate normal distribution with a mean μ and covariance Σ as follows:

$$\mu = \begin{bmatrix} 3.35 \\ 3.35 \\ 3.35 \\ 3.35 \end{bmatrix} \text{mm}, \quad \Sigma = \begin{bmatrix} 0.036^2 & 0.000 & -0.033^2 & 0.000 \\ 0.000 & 0.036^2 & 0.000 & -0.033^2 \\ -0.033^2 & 0.000 & 0.036^2 & 0.000 \\ 0.000 & -0.033^2 & 0.000 & 0.036^2 \end{bmatrix} \text{mm}^2 \quad (2)$$

where the first and third variable represents the thicknesses of two parallel walls and the second and fourth variable the thickness of the two other walls.

In order to represent the cutting process of the profiles, straight end planes at each end of the profile which is originally perpendicular to the z-axis, are defined. These planes may be rotated by an angle about the x-axis and the y-axis. These angles will be independent and normal distributed with a mean of 0° and a standard deviation of 0.25° . The end nodes will then be moved inwards or outwards in the z-direction such that they intersect these planes. Further it is reasonable that the profile will not be fixed exactly perpendicular to both the impactor and the fixation wall. Hence the profile will be given a small rotation about the x-axis and the y-axis, both with mean 0° and a standard deviation of 0.1° .

Samples from a normal distribution may range from minus infinity to plus infinity. In order to avoid unreasonable values truncated normal distributions are used. A new sample is generated if the value of a sample is more than ± 6 standard deviation from the mean. This restriction is applied to the variables concerning the angles and the thicknesses.

Simulations

The effect of varying σ^2 , ϕ and R of the covariance function σ will be investigated. In order to reduce the number of simulations it was decided to choose one length; $L = 1000$ mm. A two-level full-factorial design will be used with the levels presented in Table 3.

Table 3. The levels of each factor

Level	σ^2 [mm ²]	ϕ	R [mm]
1	0.01^2	1	20
2	0.04^2	3	40

The number of simulations per treatment combination was chosen to be 15, which resulted in $2 \times 2 \times 2 \times 15 = 120$ simulations of about 3 hours each. Each combination has been given a name, *stoc_#_#_#*, where the first, second and third number (#) represent the level of σ^2 , ϕ and R , respectively. The simulations were run in LS-DYNA version ls970 at a 16-nodes Linux cluster. The results are presented in Table 4.

Table 4. Results for each combination of the 2x2x2 factorial design.

Name	P_m		Mode		
	Mean [kN]	StDev [kN]	P [%]	T [%]	G [%]
<i>stoc_1_1_1</i>	63	11.1	27	73	0
<i>stoc_1_1_2</i>	67	10.2	13	87	0
<i>stoc_1_2_1</i>	53	14.5	7	67	27
<i>stoc_1_2_2</i>	85	4.7	60	40	0
<i>stoc_2_1_1</i>	65	8.2	20	80	0
<i>stoc_2_1_2</i>	61	8.7	20	80	0
<i>stoc_2_2_1</i>	64	11.9	33	67	0
<i>stoc_2_2_2</i>	74	16.6	67	20	13

In the first column the name of each combination is given. Then the average force P_m follows, which is found by dividing the absorbed energy by the total deformation which was 600 mm. Both the sample mean and standard deviation are presented. The percentages of the different buckling modes observed are given under *Mode*.

The percentage of the different modes changes substantially as the factorial levels changes. For most of the combinations the profiles experience progressive buckling (P) or transition from progressive to global buckling (T), while only a few samples in two of the combinations buckle globally (G). Examples of simulations of profiles which buckled in the three different modes are depicted in Figure 4, Figure 5 and Figure 6.

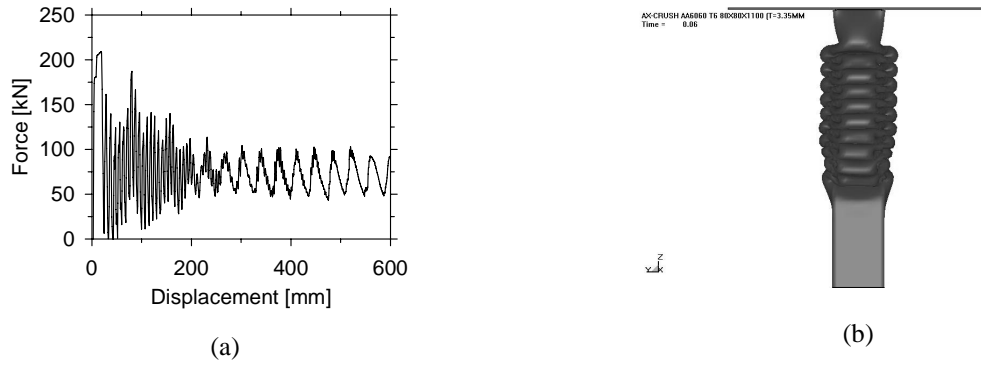


Figure 4. Progressive buckling, simulation number 6 of stoc_1_1_1: (a) force versus displacement, (b) deformation mode.

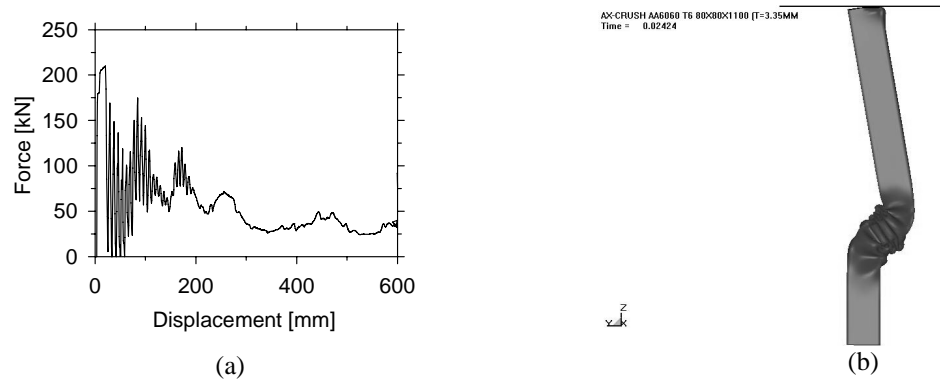


Figure 5. Transition between progressive and global buckling, simulation number 3 of stoc_2_2_1: (a) force versus displacement, (b) deformation mode.

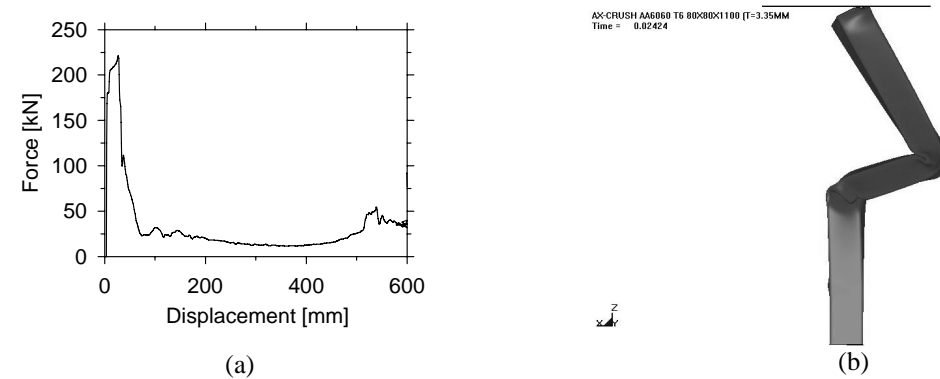


Figure 6. Global buckling, simulation number 14 of stoc_1_2_1: (a) force versus displacement, (b) deformation mode.

In Figure 4 a force-displacement curve and a picture of the deformed geometry are presented for a simulation of a profile which buckled progressively. The force-displacement curve has an initial peak followed by oscillations around a lower force-level. Figure 5 demonstrates the force-displacement curve and the deformation mode for a simulation of a profile which had a transition from progressive to global buckling. The force-displacement curve has an initial peak followed by oscillations around a lower force level, and then it drops further as the profile buckles globally. The force-displacement curve and deformation mode for a global buckling case is shown in Figure 6. The force level has an initial peak, and then it drops to a quite low force level.

In Figure 7 main effect plots of the sample mean of P_m versus the factors are shown. σ^2 is represented by its square root, called Sqrt(sill). From the figure it can be found that P_m decrease as the square root of σ^2 increases, while it increases as ϕ and R increase. For the chosen ranges of the factors, ϕ and R are the most important factors. Hence the shape of the imperfections seems to be more important than the amplitude.

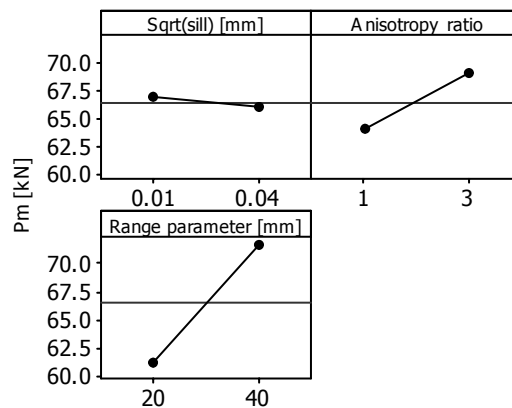


Figure 7. Main effects: average force versus the factors.

The model seems to capture the different buckling modes observed in the experiments quite well. In the experiments the profiles with L about 1000 mm buckled progressively. However, the simulations showed that a high percentage of the profiles buckled progressively for some combinations, while in other combinations most of the profiles experienced a transition mode.

Concluding Remarks

The effect of geometric variations on the impact behavior of square aluminium tubes was investigated by use of stochastic variables and assumed random fields. Variation of the random field parameters by use of a factorial design resulted in variation in especially the buckling modes and consequently the average force. Progressive buckling, global buckling and a transition from progressive to global buckling were experienced. For the chosen model the shape of the local geometric imperfections seems to be more important than the amplitude.

Other variations which have not been considered, but may be important for the behavior are spatial material variations and spatial thickness variations.

Acknowledgements

The present work has been carried out with financial support from The Norwegian University of Science and Technology.

References

- [1] Jensen Ø., Langseth M., Hopperstad O.S., Experimental investigations on the behavior of short to long square aluminium tubes subjected to axial loading, *International Journal of Impact Engineering*, 2004, vol. 3, pp. 973-1003
- [2] Jensen Ø., Behavior of aluminium extrusion subjected to axial loading, Norwegian University of Science and Technology, 2005
- [3] Marczyk J., PRINCIPLES OF SIMULATION-BASED COMPUTER-AIDED ENGINEERING, Artes Gráficas Torres, 1999
- [4] Banerjee B., Carlin B. P., Gelfand A. E., Hierarchical Modeling and Analysis for Spatial Data, Chapman & Hall/CRC, 2004
- [5] R Development Core Team. R: A language and environment for statistical computing. R Foundation for Statistical Computing, Vienna, Austria, 2004
- [6] Paulo J. R. Jr, Peter J. D., geoR: A package for geostatistical analysis. *R-NEWS*; 2001, vol. 1, pp. 14-18
- [7] Hallquist J., O. LS-DYNA Keyword User's Manual, Version 970, Livermore Software Technology Corporation, 2003
- [8] Hallquist J. O., LS-DYNA Theoretical Manual. Livermore Software Technology Corporation, 1998

